

A Study of Insulated Glazing Unit Surface Temperature Profiles Using Two-Dimensional Computer Simulation

Pedro F. de Abreu

Roydon A. Fraser, Ph.D., P.E.

Harry F. Sullivan, Ph.D., P.E.

John L. Wright, Ph.D., P.E.

Member ASHRAE

Member ASHRAE

ABSTRACT

This paper describes one part of a collaborative research project, including both measurement and simulation studies, aimed at determining the surface temperature of a set of insulated glazing units (IGUs). In this study computer simulation was used to determine the vertical surface temperature profiles of seven air-filled glazing units. Glazing system design options included variations in edge-seal type, pane spacing, low-e coating, and number of glazings. Two approaches were taken: one, a simulation of the complete problem domain using a fully detailed two-dimensional numerical simulation program (BRAVO); the second, a simplified approach using the VISION4 program for one-dimensional center-glass analysis and the FRAME 4.0 program for analysis of the remaining sections. This study serves as an important step in the development of alternative methods for evaluating condensation resistance. The present study significantly extends the database of two-dimensional simulation results. Details regarding the other parts of this project can also be found in the literature.

INTRODUCTION

This paper describes one part of a collaborative research study aimed at determining the surface temperature of a set of insulated glazing units (IGUs). Both measurement and simulation are included in this effort. Duplicate sets of glazing units were provided to the measurement laboratories and their construction details were given to the simulation laboratories. Thermocouple-based techniques have been developed for measuring the condensation resistance of windows (Elmahdy 1990). This study serves as an important step in the development of alternative methods for evaluating condensation resistance. All participants in the study were asked to perform their portion of the research without knowledge of the results of the other investigators, i.e., a "blind study." A more complete description

of this collaboration among four laboratories is given by Sullivan et al. (1996).

This paper focuses on determining by simulation a priori (i.e., before any corresponding computational or experimental data are available) the vertical surface temperature profiles of the seven air-filled glazing units identified in Table 1. The numbering scheme shown in Table 1 will be used throughout the paper to identify the glazing units. The design options incorporated in these glazing units were selected to cover a range (i.e., edge-seal type, pane spacing, low-e coating, number of glazings) that would test both the measurement and simulation techniques. These same design options are of interest because each one affects the indoor surface temperature profile.

TABLE 1 Description of Air-Filled Glazing Units

IGU#	Glass Description	Individual Pane Spacing(s), <i>d</i>	Spacer(s)
1	Clear double-glazed	12.7 mm (0.50 in.)	Foam
2	Clear double-glazed	12.7 mm (0.50 in.)	Aluminum (single seal)
3	Clear double-glazed	6.4 mm (0.25 in.)	Foam
4	Clear double-glazed	19.1 mm (0.75 in.)	Foam
5	Low-e double-glazed	12.7 mm (0.50 in.)	Foam
6	Clear triple-glazed	12.7 mm (0.50 in.)	Foam
7	Clear triple-glazed	6.4 mm (0.25 in.)	Foam

Pedro F. de Abreu is a graduate student, Roydon A. Fraser is an associate professor, Harry F. Sullivan is a professor, and John L. Wright is an adjunct professor in the Mechanical Engineering Department at the University of Waterloo, Waterloo, Ont., Canada.

The primary objective of this paper is to report vertical, centerline surface temperature profiles generated using the two-dimensional convection/conduction/radiation computational code BRAVO (de Abreu 1995). A second set of simulation results was produced using VISION and FRAME. These computer programs are widely used for center-glass (one-dimensional) and frame and edge-glass (two-dimensional) simulation, respectively. The most recently released versions, VISION4 and FRAME 4.0, include simple extensions that account for fill-gas convection (Wright and Sullivan 1995; McGowan 1995a, 1995b). This simplified convection model allows for the evaluation of condensation resistance without undertaking a detailed simulation of a full window.

The goal of determining surface temperature profiles is more challenging than the traditional exercise of comparing U-factors because local, rather than averaged, results must be found. Therefore, this research project serves the additional purpose of highlighting the capabilities and limitations of current window simulation techniques. Conclusions that do not require comparison with collaborative laboratory data are presented. Conclusions based on a comparison with data from collaborating laboratories are given by Sullivan et al. (1996).

GLAZING UNIT DETAILS AND MOUNTING CONFIGURATION

The double-glazed units identified in Table 1 involving the foam spacer are modeled as shown in Figure 1a. The triple-glazed units are modeled similarly. The pane spacing, d , shown in Figure 1 is given in Table 1.

Details regarding the metal spacer modeled are shown in Figure 1b. The metal is aluminum. A 50- μm air gap is used to simulate the solid-solid thermal contact resistance that exists between the glazing and the aluminum spacer (Fraser et al. 1993). The spacer model is a simplification of the true spacer geometry with the thickness of the aluminum preserved, as Fraser et al. (1993) show that it is the metal thickness and not the spacer's shape that dominates edge-seal thermal performance.

IGU 5 has a low-e coating (emissivity ≈ 0.2) on the indoor-facing surface of the outdoor glazing (surface 2). The emissivity of the glass is taken as 0.84.

It is worth noting that the test samples are IGUs mounted in a mask wall without a sash or frame. The advantage of this simple arrangement is the removal of complicating factors. The disadvantage, however, is that the reader must keep in mind, for instance, that sensitivities to edge-seal structure may be magnified. In particular, the edge-seals of the glazing units studied account for a greater percentage of the heat loss than they would if a sash were present.

The tape shown in Figure 1a was necessary in the experiment to fasten the glazing in place and to prevent infiltration. The tape, however, was not modeled because it was felt that its presence would not alter the heat transfer appreciably.

SIMULATION CONDITIONS

The boundary conditions used for computer simulation are listed in Table 2. The heat transfer coefficients include both longwave radiation and convective effects. No solar radiation is present. These boundary conditions approximate the ASHRAE winter design condition, with a 15-mph (6.7-m/s) wind on the cold side and natural convection on the warm side, but were chosen with the expectation that they would also approximate the conditions found in the measurement laboratories. This paper includes a brief sensitivity study to variations in the magnitudes of these coefficients. This information is important when comparing computational and experimental results.

Also note that h_o and h_i were modeled as constant (i.e., independent of position along the exposed glazing surface). This may not be representative of local film coefficient variations, particularly on the indoor side, where peculiarities in the boundary-layer flow near the head and sill are expected. In this study the test units were mounted flush on the warm side to minimize this effect.

SIMULATION CODES

BRAVO—Two-Dimensional Glazing/Frame/Wall Thermal Performance Code

BRAVO, a nonorthogonal grid, control-volume-based computational code developed specifically for the two-dimensional modeling of window assemblies, is utilized in this paper (de Abreu 1995). One strength of the code is its ability to model an entire window assembly (center-glass, edge-glass, frame, wall) simultaneously. This is in contrast to the current industry practice of modeling the center-glass region separately from the edge-glass/frame/wall region (EEL 1995; UW 1995; LBL 1994) as practiced by the Canadian Standards Association's (CSA) window energy rating (ER) procedure (CSA 1993) and the National Fenestration Rating Council's (NFRC 1991) procedure.

BRAVO was selected for this work for several reasons. It incorporates much of the appropriate physics, it yields detailed surface temperature profiles, and it provides flexible boundary condition capabilities. For example, no assumption concerning the location of edge-glass demarcation is needed; a detailed vertical temperature profile along the entire window is available for comparison with thermographic measurements; and specification of an indoor window surface temperature or heat transfer coefficient can be replaced with room air convection.

The ability of BRAVO to accurately determine local window temperatures makes it possible to better address local window performance problems such as condensation (Wright and Sullivan 1995; McGowan 1995a, 1995b). Although not central to this paper, an accurate code may also be used to supplement experimental data in validating simpler, more user-friendly codes (EEL 1995; UW 1995).

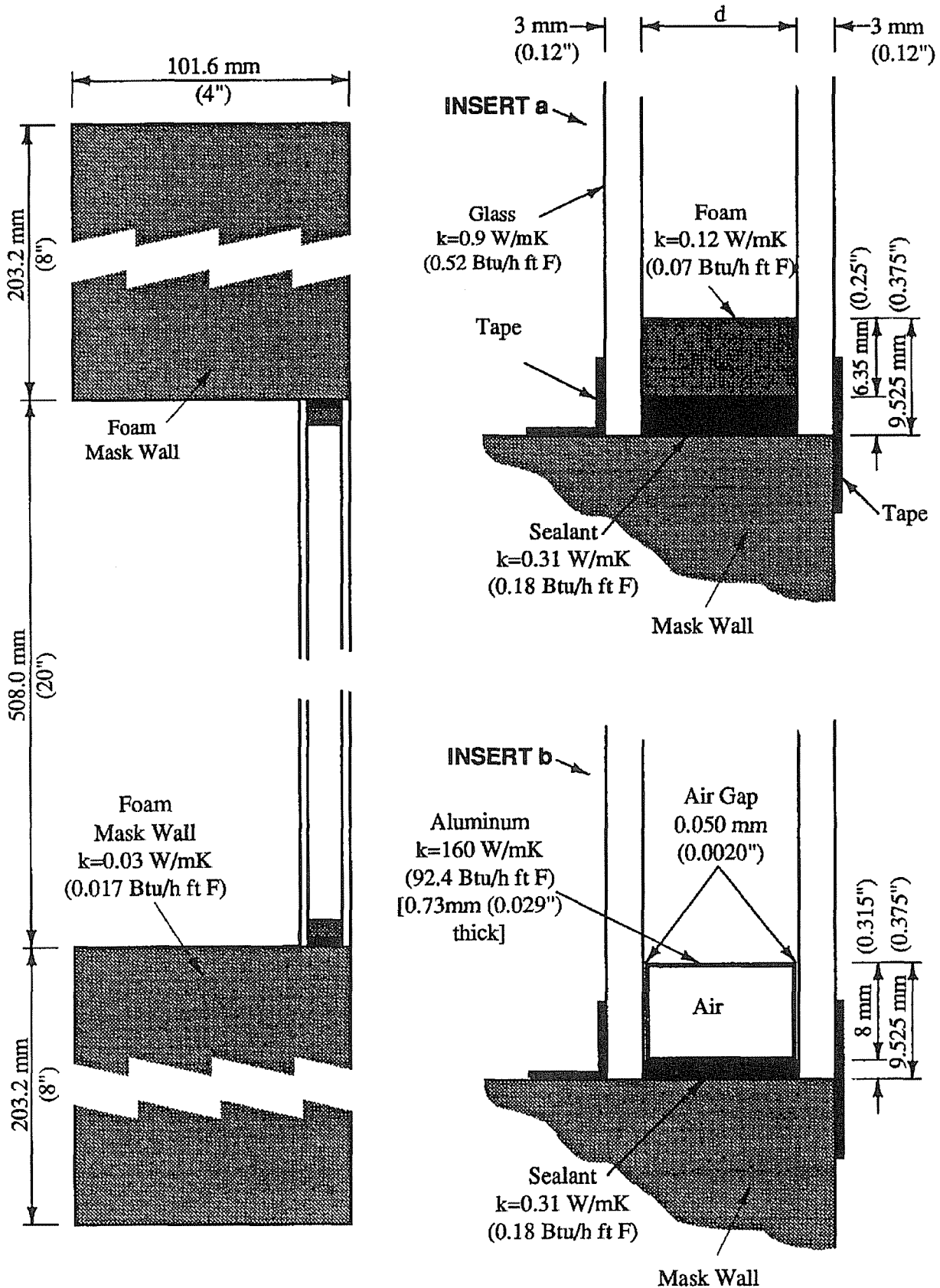


Figure 1 Glazing unit and mask wall geometry.

TABLE 2 Glazing Unit Boundary Conditions

Indoor Temp. T_i	Indoor Heat Transfer Coefficient h_i	Outdoor Temp. T_o	Outdoor Heat Transfer Coefficient h_o
21.1°C	8.3 W/m ² ·°C	-17.8°C	30 W/m ² ·°C
70°F	1.46 Btu/h·ft ² ·°F	0°F	5.29 Btu/h·ft ² ·°F

BRAVO Capabilities

There are seven features that together distinguish BRAVO from other computational fluid dynamics (CFD) codes. They are as follows:

1. It can model thermal radiation, convection, and conductive heat transfer in multiple cavities simultaneously. The governing equations conserving mass, momentum, and energy are all solved. It does not require, for instance, an effective conductivity or convective heat transfer correlations.
2. It can model in a simple fashion the impact of solar radiation.
3. Boundary conditions and system boundaries can readily be changed. This includes the ability to input spatially varying boundary conditions.
4. It can model secondary flow (cat's eye cells) (Wright and Sullivan 1989; Lee and Korpela 1983), expected for many combinations of IGU design and indoor-outdoor temperature combinations.
5. It can model the specular reflection of solar radiation within rectangular cavities. This feature is needed to model the real-life situation of incident solar radiation striking a window from an off-normal direction.
6. It can model nonorthogonal structures. This feature is useful for modeling frames or for modeling deflected glazings.
7. It can be run on a personal computer with 16 Mb of memory. Runtimes in this work, using a 66-MHz processor, ranged from five minutes for IGU 1 to about 90 minutes for IGU 2.

An additional feature of BRAVO that will prove useful in future work includes its ability to model windows with internal obstructions such as grilles and muntin bars.

A major limitation of BRAVO is that it is a research tool and not readily adapted for widespread commercial use by the window industry. It lacks a user-friendly interface.

Secondary Cells

A few comments about secondary cells are in order, as their influence will be seen in the simulation results for IGU 4, the double-glazing unit with 19.1-mm (0.75-in.) pane spacing.

Four flow regimes can be identified for tall, vertical glazing cavities as a function of Rayleigh number, Ra (Wright and Sullivan 1989; Eckert and Carlson 1961). As Ra increases (i.e., increased temperature difference or pane spacing), the flow

progresses through conduction, transition, and boundary layer regimes (all laminar), eventually giving way to unsteady flow and turbulence. It has been observed that a secondary flow of regularly spaced cat's eye cells can exist in the core of the primary laminar flow if Ra exceeds about 6,000 (Bergholtz 1978). These secondary flows may be stable or unstable (Lauriat and Desrayaud 1985; Pignatell and Marcillat 1986; Chikhaoui et al. 1988).

The importance of secondary cells with respect to code validation is critical as they can lead to complex window surface temperature profiles. In effect, if a code can correctly capture these more complex temperature profiles then confidence in that code's ability to model windows is increased substantially. The validity of incorporating secondary cells has already been confirmed by comparison with measured heat transfer rates (Wright and Sullivan 1994).

For numerical reasons, cells do not always appear when modeling a flow that supports secondary flows. Consequently, it is necessary to perturb cavity flows at an intermediate stage before allowing the program to converge to a solution. If the perturbations die out in the course of convergence, then the flow does not support secondary cells. All glazing cavities expected to support secondary cells were so perturbed.

State-of-the-Art Window Simulation Codes

Two available programs, VISION4 (UW 1995) and FRAME 4.0 (EEL 1995), when used together can model the nonsymmetrical temperature profiles found to differentiate a window assembly's sill from head regions. VISION4 calculates a window's center-glass performance, while FRAME 4.0 focuses on the thermal performance of a window's edge-glass and frame regions. Together these programs can yield an estimate of the overall thermal performance of a given window assembly (CSA 1993). All VISION4/FRAME 4.0 simulations reported in this paper incorporate the convection option, i.e., the convective flow field within the glazing cavity is calculated first by VISION and then passed to FRAME for subsequent use (Wright and Sullivan 1995).

Simulations using VISION4/FRAME 4.0 require two steps (EEL 1995). First, VISION4 is used to complete a one-dimensional center-glass analysis yielding glazing temperatures and rates of heat transfer. This one-dimensional calculation is based largely on fundamental principles but must rely on correlations to estimate rates of convective heat transfer. Second, FRAME 4.0 is used to complete a numerical two-dimensional edge-glass and frame analysis using information taken from the VISION4 results to assign an "effective conductivity" to the fill gas. The use of an effective conductivity enables the two-dimensional solution to be generated without accounting for fill gas convection, but the solution generated in this fashion carries no information about the local effects of fill gas motion. The VISION4/FRAME 4.0 software can be run in a second mode that accounts for fill gas motion in a simplified manner. In this case, VISION4 runs a two-dimensional calculation to determine the fill gas velocity field in each glazing cavity by modeling the vertical side

walls as isothermal. The temperatures of these side walls are known from the previous one-dimensional calculation. The velocity of the fill gas in the edge-glass region and the temperature of the fill gas entering the edge-glass region are then stored for use by FRAME 4.0. FRAME 4.0, run in its convection mode, can then generate an edge-glass and frame solution that accounts for the effect of fill gas motion. The second mode of VISION4/F RAME 4.0 operation (i.e., convection mode) was developed with the intention of making condensation resistance evaluation available with the same level of expediency that the more conventional VISION4/F RAME 4.0 runs provide.

The VISION4/F RAME 4.0 results presented in this paper include the VISION4 center-glass surface temperatures taken from the one-dimensional calculation plus head and sill surface temperature profiles generated using F RAME 4.0 in its convection mode. Note that F RAME 4.0, run in its convection mode, will not allow the user to specify an edge glass region different from 63.5 mm (2.6 in.). Plots presented later will show a discontinuity at this location.

SIMULATION RESULTS

The graphical presentation of the simulation results is similar for all of the glazing units. The vertical axis represents vertical distance with zero corresponding to the bottom edge of the glazing unit and the top edge at 508 mm (i.e., 20-in. glazing dimension). The vertical axis runs from -100 mm to +600 mm so that 100 mm of the foam mask wall is shown both below and above the glazing unit. The horizontal axis records the temperature profile in degrees Celsius on the warm side (room side) of the glazing unit. This temperature profile represents any vertical profile along the glazing unit as long as the "side effects" of the spacer and sealant, etc., are not influencing the temperature. The glazing units tested and simulated were 356 mm by 508 mm (14 by 20 in.), and previous IR thermographic data (Sargent 1994) have indicated that a major portion of the glazing unit can be expected to be free of side effects (e.g., corner effects were confined to a relatively small region in the vicinity of the corners). In the comparison with experimental data, these simulated temperature profiles will be compared with the vertical temperature profiles measured along the centerline of the glazing units.

Reference Glazing Unit

Glazing unit 1, a clear double-glazed unit with a 12.5-mm (0.5-in.) air cavity and a foam edge-seal, can be considered a reference unit. The remaining six glazing units contain a number of variations from this reference configuration and the presentation of the simulation results will typically contrast the effects of these physical variations on the temperature profile of the glazing unit in question relative to the reference glazing unit.

Composite Results

Figure 2 is a composite plot showing the temperature profiles for all seven glazing units. Most figures are plotted to the

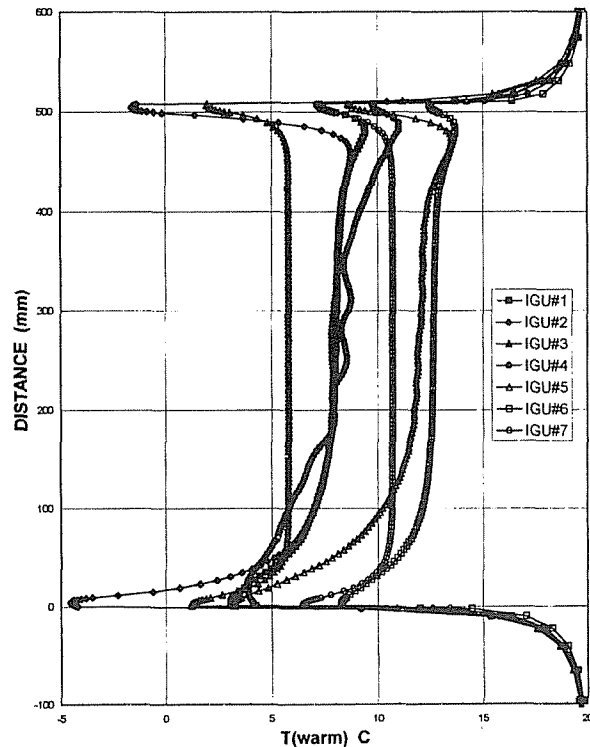


Figure 2 Warm-side temperature profile for all seven glazing units (BRAVO only).

same temperature scale to facilitate both qualitative and quantitative comparison.

In Figure 2 it is relatively easy to sort out the different temperature profiles on the basis of their center-glass heat transfer characteristics. For example, in the midpart of the graph, away from the top and bottom edge effects, the lowest performing unit is the double-glazed 6.35-mm (0.25-in.) unit (IGU 3), and the best performing units are the clear triple unit with the largest spacings (IGU 6—two 12.7-mm [0.5-in.] air cavities) and the 12.7-mm (0.5-in.) low-e unit (IGU 5). The remaining units occupy positions consistent with intuition. A comparison of the simulated center-glass temperatures from this study with those predicted by VISION4 (UW 1995) is shown in Table 3. There is good agreement for all seven IGUs, with the greatest discrepancy for IGU 4, in which the waviness caused by secondary cells in the fill-gas flow makes comparison difficult. In the other six units, the BRAVO midpoint temperatures agree with the corresponding VISION4 indoor glass temperatures to within several tenths of one degree Celsius. Although the relative ordering of the profiles fits intuition, there are a number of other features that would not have been obvious before performing the two-dimensional simulations. These more detailed observations are best shown with other figures.

Figure 3 is a comparison of the temperature profiles for two glazing units identical in all respects except for the spacer. IGU 1 has a 12.7-mm (0.5-in.) foam spacer and IGU 2 has a 12.7-mm

TABLE 3 Thermal Performance Characteristics of the Glazing Units

IGU	U-Factor	R-Value	Center-Glass Temperature		
	W/m ² ·°C (Btu/h·ft ² ·°F)	m ² ·°C/W (h·ft ² ·°F/Btu)	°C (°F)		
	VISION4	VISION4	BRAVO	VISION4	Difference
1	2.87 (0.51)	0.35 (1.98)	8.03 (46.5)	7.66 (45.8)	0.37 (0.7)
2	2.87 (0.51)	0.35 (1.98)	7.84 (46.1)	7.66 (45.8)	0.18 (0.3)
3	3.28 (0.58)	0.30 (1.73)	5.79 (42.4)	5.72 (42.3)	0.07 (0.1)
4	2.91 (0.51)	0.34 (1.95)	8.55 (47.4)	7.48 (45.5)	1.07 (1.9)
5	2.05 (0.36)	0.49 (2.76)	11.88 (53.4)	11.47(52.6)	0.41 (0.8)
6	1.84 (0.32)	0.54 (3.08)	12.65(54.8)	12.48 (54.5)	0.17 (0.3)
7	2.23 (0.39)	0.45 (2.54)	10.72(51.3)	10.66 (51.2)	0.06 (0.1)

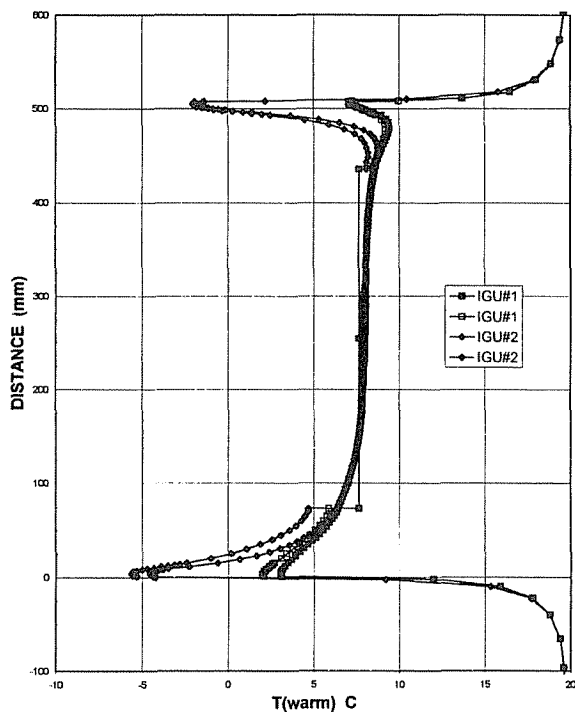


Figure 3 Effect of spacer material, foam vs. metal, IGUs 1 and 2 (BRAVO-closed symbols, VISION4/FRAME 4.0-open symbols).

(0.5-in.) aluminum spacer bar. Both units have also been modeled with appropriate amounts of sealant material. The model used for the aluminum spacer bar configuration incorporates a narrow air gap (50 microns) to simulate the effects of the contact resistance that occurs at the glass-metal interface. For details about edge-seal modeling, the reader is referred to Fraser et al. (1993) and Wright et al. (1994) in which a detailed comparison of spacer simulation models and experimental measurements was carried out. The VISION4/FRAME 4.0 simulation results are in good agreement with the results from the two-

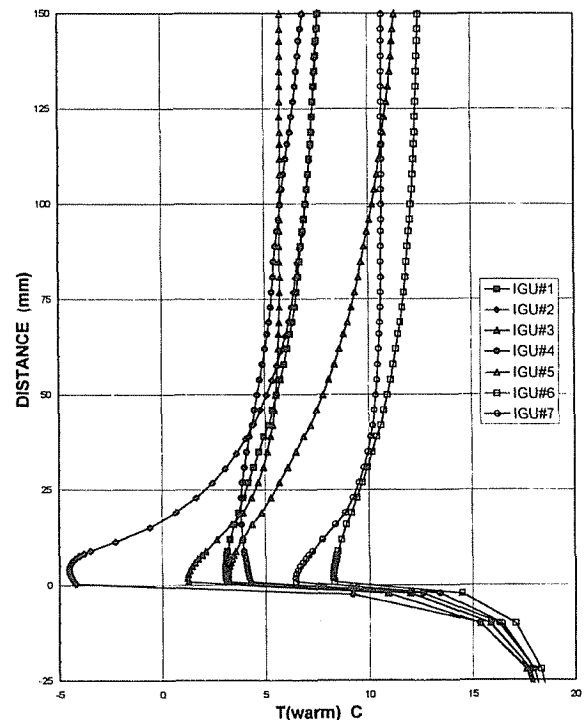


Figure 4 Enlarged plot of temperature profiles near bottom edge (BRAVO only).

dimensional simulation BRAVO. At the sill section, the temperatures differ by approximately 1°C for both IGUs 1 and 2. At the head section, the two simulation results are virtually identical. Across the center-glass region, the constant value from the one-dimensional VISION4 simulation is an excellent representation of the average temperature across this portion of the glazing.

As expected, the unit with the aluminum spacer bar shows significantly lower temperatures than the unit with the foam spacer at both the head and sill regions. Across the center of the glazing unit, the temperature profiles are essentially identical.

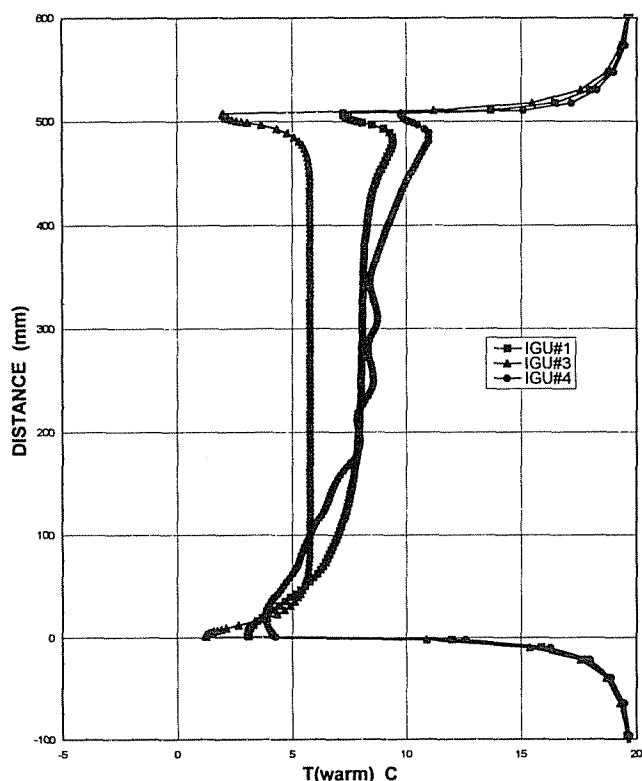


Figure 5 Effect of pane spacing IGUs 1, 3, and 4 (BRAVO only).

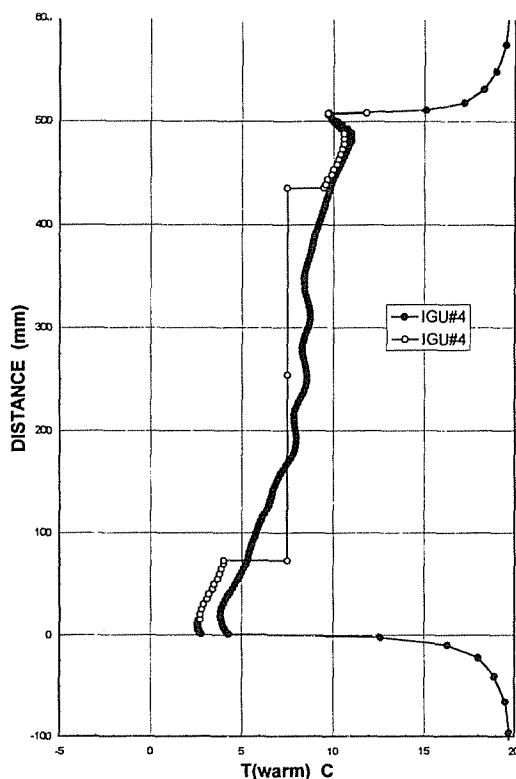


Figure 6 Wide pane spacing with secondary fill gas flow, IGU 4 (BRAVO-closed symbols, VISION4/FROME 4.0-open symbols).

The region of departure from the temperature profile of reference unit IGU 1 is on the order of 50 mm (2 in.) at the top and 75 mm (3 in.) near the bottom. Since most attention is usually focused on the sill portion near the lower sightline, an enlarged plot of this region for all seven glazing units is shown in Figure 4. Once again, the qualitative features illustrated in this figure can be easily explained. The coldest temperature is for the metal spacer, with the next coldest being the narrow-gap (6.75-mm [0.25-in.]) foam spacer. The two units with 12.7-mm (0.5-in.) foam show an incremental improvement, as does the unit with the 19.1-mm (0.75-in.) foam spacer. Both triple-glazed units show the increased benefits of the longer path lengths through the foam spacer constituting the thermal bridge as well as the incremental resistance provided by the additional pane of glass. Because all of these units are glazing units only, without a sash or frame, the reader is cautioned not to generalize these results to complete windows.

Effect of Pane Spacing

Figure 5 shows the temperature profiles for IGU samples 1, 3, and 4. These three glazing units are identical except for the thickness of the air cavity (and the corresponding foam spacer). The three spacings represented are 6.75, 12.7, and 19.1 mm (0.25, 0.5, and 0.75 in.). This figure contains some results that might not have been expected. The temperature profile for IGU 3 is significantly

“flatter” across the center-glass region. Although the midpoint temperatures for both units 1 and 4 are similar (an expected result since we know that beyond a spacing of 12.7 mm [0.5 in.] there is little additional benefit to going to larger spacings), these two temperature profiles have different characteristic shapes. The slope changes progressively from the 6.75-mm (0.25-in.) to the 12.5-mm (0.50-in.) and finally to the 19.1-mm (0.75-in.) unit as a consequence of the changing convective flow in the cavity. The mechanism of convective heat transfer shifts from conduction to boundary layer transport as the aspect ratio of the glazing cavity increases. The temperature profile for IGU 4 also exhibits characteristics of the secondary flow (“cat’s eye cells”) that is present (Wright and Sullivan 1989, 1994).

The temperature profile for IGU 4 is replotted in Figure 6, where the VISION4/FROME 4.0 simulation results are compared. It can be seen that the effect of fill gas motion at the extremities of the IGU is picked up by the simplified VISION4/FROME 4.0 analysis, but the one-dimensional VISION4 calculation does not provide detail through the center-glass region. However, it should be noted that the test units are relatively short (in this case, cavity aspect ratio = $508/19.1 \approx 17$). Units with high aspect ratios display a flatter center-glass temperature profile that can be represented more readily with a one-dimensional calculation.

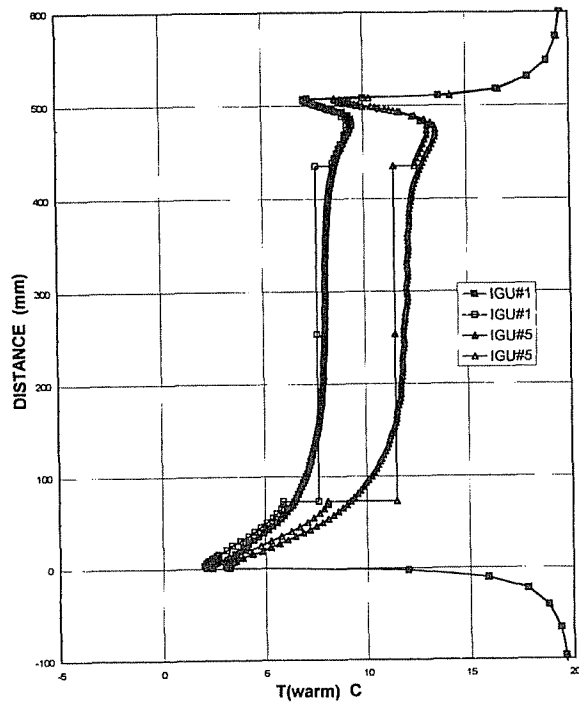


Figure 7 Effect of low-e coating, IGUs 1 and 5 (BRAVO-closed symbols, VISION4/FRAME 4.0-open symbols).

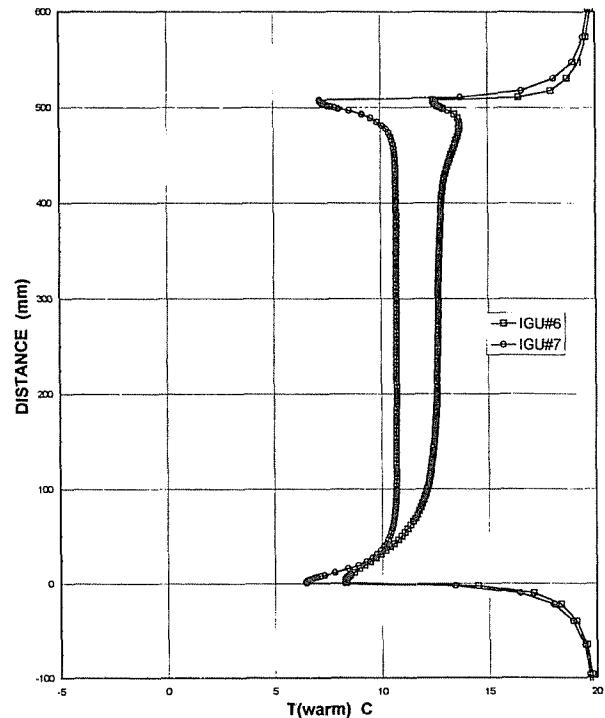


Figure 8 Comparison of triple-glazed units, IGUs 6 and 7 (BRAVO only).

Effect of Low-e Coating

Figure 7 shows the temperature profiles for IGU samples 1 and 5, two glazing units identical in all respects except for the presence of a low-e coating (modeled with an emissivity of 0.20) on surface 2 (the cavity side of the outdoor or cold-side pane). The main observation is that the presence of the low-e coating reduces the overall heat transfer through the glazing unit, resulting in significantly warmer temperatures on the warm side except at the edges of the glazing, where the glazing units have identical 12.7-mm (0.5-in.) foam spacers. Clearly, the effect of higher center-glass thermal resistance does not extend to the edge-of-glass region. Improved spacer designs must accompany the enhanced center-glass features.

The effect of the thermal bridge and the superimposed convective effect persists for a significant distance away from the lower edge, up to as much as 150 mm (6 in.), and at the top, the “edge effect” appears to be present for a dimension on the order of 100 mm (4 in.).

Triple-Glazed Units

Figure 8 shows the temperature profiles for the two triple-glazed units (IGU 6 with two 12.7-mm [0.5-in.] cavities, and IGU 7 with two 6.75-mm [0.25-in.] cavities). In Figure 8 it can be seen that the profile shapes through the center-glass differ because of the difference in cavity

aspect ratios. The unit with the high aspect ratio (i.e., narrower pane spacing) has a flatter curve. The same observation was made regarding the various double-glazed units. Another observation from Figure 8 is, as expected, that IGU 6 has a higher edge-glass temperature than IGU 7 because of the longer thermal path through the thicker spacers.

A variety of interesting observations can be made in comparing the bottom edge temperatures of the triple-glazed units vs. IGU 5—the double-glazed low-e unit with 12.7-mm (½-in.) pane spacing. The center-glass temperatures of these three units are similar, but the bottom-edge temperatures of the triple-glazed units are higher because of the additional conduction path length and also because the intermediate pane deflects the convective fill-gas flow.

Figure 9 shows results for IGU 6 replotted along with the corresponding VISION4/FRAME 4.0 results, showing that the simplified code provides the same level of agreement demonstrated in the analysis of double-glazed units.

Bottom Edge Surface Temperature Prediction

Examination of Figures 3, 6, 7, and 9 reveals that the temperature profiles and minimum surface temperatures predicted by the simplified VISION4/FRAME 4.0 analysis are in good agreement with BRAVO results. The minimum temperature predictions differ at most by about 1°C (33.8°F), but it can also be noted that the minimum temperature generated by the

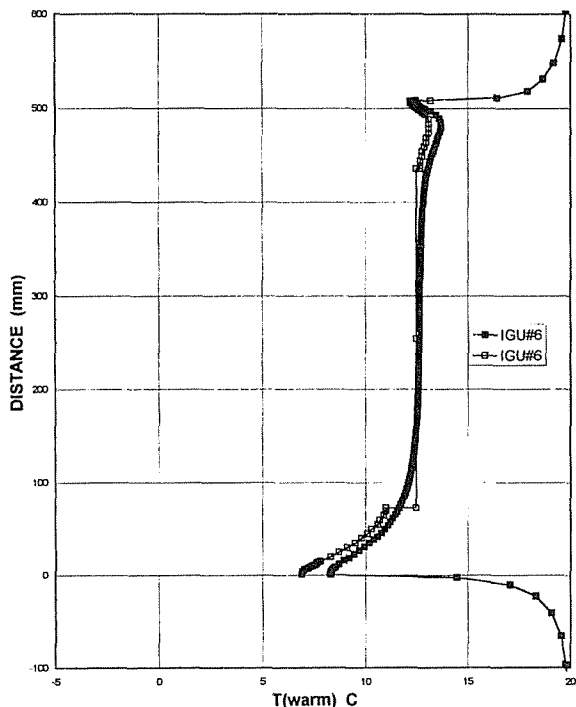


Figure 9 Triple glazing with 12.7-mm (.5-in.) pane spacing, IGU 6 (BRAVO-closed symbols, VISION4/FROME 4.0-open symbols).

simplified analysis is consistently lower than the BRAVO result. It is felt that this is a consequence of the approximate nature of the fill-gas velocity field supplied by VISION4. This velocity field is determined for the situation where the center-glass temperatures of the bounding walls extend fully to the top and bottom of the glazing cavity. In reality, the bottom extremity of the indoor glazing will be colder. Thus, the boundary layer forming in the fill gas next to this section of glass under the approximate isothermal wall condition will develop more quickly, will be thinner, and will entail higher temperature gradients. Consequently, the approximate flow field can be expected to provide additional cooling to the bottom edge of the indoor glazing and consistently give conservative estimates of minimum indoor surface temperature.

SENSITIVITY ANALYSIS

At the outset of this investigation, it was clear that although several testing laboratories would attempt to test identical sets of glazing units at the same test conditions, physical differences in the laboratories would invariably lead to different boundary conditions. For example, one laboratory uses a perpendicular wind direction whereas the other laboratory uses a parallel wind direction with the flow from bottom to top. In addition, there are other differences associated with the presence or absence of constant-temperature radiation baffles. These differences are expected to influence the cold-side and warm-side film coefficients, designated h_o and h_i , respectively. Note that these are total

heat transfer coefficients combining both the convective and radiative components. The nominal test conditions were to reproduce forced convection of 6.7 m/s (15 mph) on the cold side and natural convection on the warm side. Typically this would result in coefficients of h_o up to 34 W/m²·°C (6.0 Btu/h·ft²·°F) and h_i of 8.3 W/m²·°C (1.46 Btu/h·ft²·°F). To have "simulation conditions" match "test conditions," discussion with one of the researchers fixed these coefficients at 30 and 8.3 W/m²·°C, respectively. The results shown in all figures correspond to these fixed film coefficients.

Figures 10 and 11 are indications of the effect on the indoor surface temperature profile for the reference glazing (IGU 1) of changes in h_i in increments (6, 7, 8, and 9 W/m²·°C) for a fixed h_o of 30 W/m²·°C and changes in h_o in increments (10, 20, 30, and 40 W/m²·°C) for a fixed h_i of 8 W/m²·°C. Figure 11 shows that beyond a value of $h_o = 30$ W/m²·°C, little additional effect is expected and that in the range from 10 to 30 the major qualitative effect is a shift in the temperature profile, with the profile shape remaining unchanged. Figure 10 shows that variations in h_i in the range from 6 to 9 also shift the profile but preserve the profile similarity. Although the simulations were performed with constant values of h_o and h_i (with respect to location), neither the test conditions nor the real-world installation geometry (sash and frame components, sills, recessed windows, etc.) is likely to yield uniform film coefficients. This invariably will lead to differences between simulations and measurements (Sullivan et al. 1996), the extent of which can only be determined by the data comparison that this research study set out to accomplish.

CONCLUSIONS

Although simulations of the top to bottom temperature profiles for a few specific windows have been reported in the literature, this study represents the first attempt to perform a systematic variation of glazing properties on a set of glazing units measured and simulated in a "blind" comparison test. This is an important study for that reason.

Although one-dimensional analysis for the center-glass region and two-dimensional conduction analysis for the edge-glass and frame regions have been common practice for several years, complete two-dimensional simulations had previously been reported by only one or two researchers and then only for a narrow range of glazing properties and temperature conditions. The present study significantly extends the database of two-dimensional simulation results.

It is apparent that the simplified VISION4/FROME 4.0 convection analysis is a valuable tool for estimating the indoor surface temperatures near the bottom edge of an IGU where condensation problems are most severe. In general, the minimum indoor glazing surface temperatures given by BRAVO were reproduced by VISION4/FROME 4.0 to within about 1°C.

ACKNOWLEDGMENTS

The Advanced Glazing System Laboratory is supported by CANMET (Natural Resources Canada) and the Natural Sciences and Engineering Research Council of Canada. The

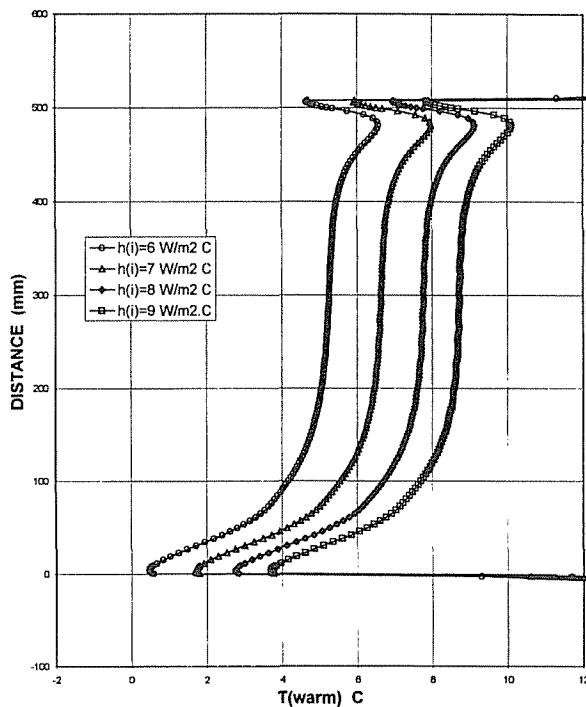


Figure 10 Sensitivity analysis: Effect of changes in h_i with h_o fixed at $30 \text{ W/m}^2 \cdot ^\circ\text{C}$ IGU 1 (BRAVO only).

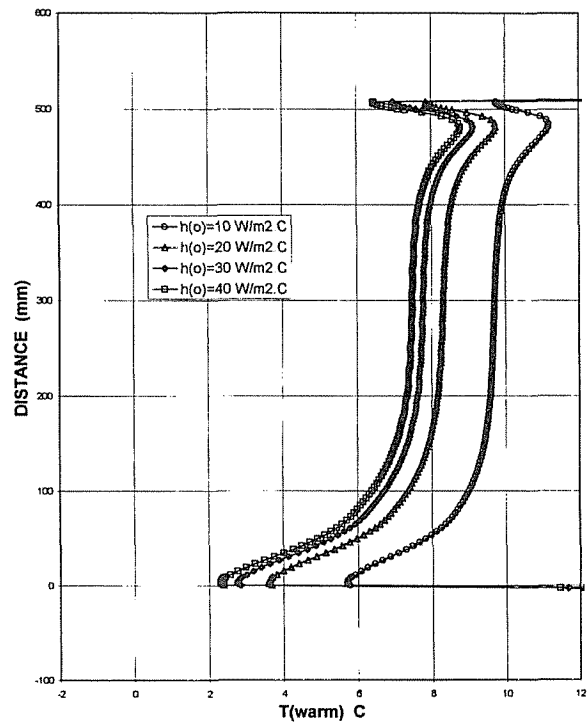


Figure 11 Sensitivity analysis: Effect of changes in h_o with h_i fixed at $8 \text{ W/m}^2 \cdot ^\circ\text{C}$ IGU 1 (BRAVO only).

authors wish to thank Dave Sargent (Edgetech I.G.) for fabricating the IGU test samples and supplying details regarding their geometry for simulation.

REFERENCES

- Bergholtz, R.F. 1978. Instability of steady natural convection in a vertical fluid layer. *Journal of Fluid Mechanics* 84(2): 743-768.
- Chikhaoui, A., J.F. Marcillat, and R.L. Sani. 1988. Successive transitions in thermal convection within a vertical enclosure. *Natural Convection in Enclosures*, ASME HTD 99: 29-35. New York: American Society of Mechanical Engineers.
- CSA. 1993. *CSA A440.2, Energy performance of windows and sliding glass doors*. Rexdale, Ont.: Canadian Standards Association.
- de Abreu, P. 1995. BRAVO—A full convection/conduction/radiation PC based computer code for modeling windows. Draft Ph.D. Thesis. Waterloo, Ont., Canada: University of Waterloo.
- Eckert, E.R.G., and W.O. Carlson. 1961. Natural convection in an air layer enclosed between two vertical plates with different temperatures. *International Journal of Heat and Mass Transfer* 2: 106-120.
- EEL. 1995. FRAME: A computer program to evaluate the thermal performance of window frame systems—Version 4.0. Waterloo, Ont., Canada: Enermodal Engineering Ltd.
- Elmahdy, A.H. 1990. A universal approach to laboratory assessment of the condensation potential of windows. *Proc. 16th Annual Conference of the Solar Energy Society of Canada Inc.*, Halifax, pp. 165-173, June 18-20.
- Fraser, R.A., P.F. de Abreu, J.L. Wright, H.F. Sullivan, and H. Yao. 1993. Critical issues in comparing edge-seal performance: Modeling vs. experiment. *ASHRAE Transactions* 99(): 923-938.
- Lauriat, G., and G. Desrayaud. 1985. Natural convection in air-filled cavities of high aspect ratios: Discrepancies between experimental and theoretical results. National Heat Transfer Conference, ASME.
- LBL. 1994. WINDOW 4.1: A PC program for analyzing window thermal performance in accordance with standard NFRC procedures—Program description. Berkeley, Calif.: Windows and Daylighting Group, Lawrence Berkeley Laboratory.
- Lee, Y., and S.A. Korpela. 1983. Multicellular natural convection in a vertical slot. *Journal of Fluid Mechanics* 126: 91-121.
- McGowan, A. 1995a. Numerical prediction of window condensation potential. *ASHRAE Transactions* 101(1).

- McGowan, A. 1995b. Second-generation tools for simulating window performance. *Windows Innovations '95 Conference*, Toronto, pp. 439-444.
- NFRC. 1991. NFRC 100-91, Procedure for determining fenestration product thermal properties (currently limited to U-values). Revised June 28, 1991. Silver Spring, Md.: National Fenestration Rating Council.
- Pignatelli, J.F., and J.F. Marcillat. 1986. Transition to time-dependent free convection in an inclined air layer. *International Journal of Heat and Fluid Flow* 7: 169-178.
- Sargent, D. 1994. Personal communication.
- Sullivan, H.F., J.L. Wright, and R. Fraser. 1996. Overview of a project to determine the surface temperatures of insulated glazing units: Thermographic measurement and 2-D simulation. Submitted for review. *ASHRAE Transactions* 102(2).
- UW. 1995. VISION4 computer program. Waterloo, Ont., Canada: University of Waterloo, Advanced Glazing Laboratory.
- Wright, J.L., P.F. de Abreu, R.A. Fraser, and H.F. Sullivan. 1994. Heat transfer in glazing system edge-seals: Calculations regarding various design options. *ASHRAE Transactions* 100(1).
- Wright, J.L., and H.F. Sullivan. 1989. Natural convection in sealed glazing units: A review. *ASHRAE Transactions* 95(1).
- Wright, J.L., and H.F. Sullivan. 1994. A 2-D numerical model for natural convection in a vertical, rectangular window cavity. *ASHRAE Transactions* 100(2).
- Wright, J.L., and H.F. Sullivan. 1995. A simplified method for the numerical condensation resistance analysis of windows. *Windows Innovations '95 Conference*, Toronto, pp. 429-438.